Dalton Transactions

ROYAL SOCIETY OF CHEMISTRY

PAPER

View Article Online
View Journal

Cite this: DOI: 10.1039/d0dt03124k

Ditopic bis(*N*,*N*′,*N*′-substituted 1,2-ethanediamine) ligands: synthesis and coordination chemistry†

Andreas Rösch,[a] Christoph M. Herzog,[a] Simon H. F. Schreiner,[a] Helmar Görls[b] and Robert Kretschmer *[b,c]

Received 7th September 2020,
Accepted 23rd September 2020

DOI: 10.1039/d0dt03124k

rsc.li/dalton

The synthesis of two different types of bis(*N*,*N*′,*N*′-substituted 1,2-ethanediamine)s, bridged either through the secondary (type **1**) or tertiary (type **2**) amine groups is reported. Selected protio-ligands have been applied in subsequent metallation reactions using aluminium, magnesium, tin, and zinc sources allowing to isolate five mononuclear and eight dinuclear complexes. All complexes have been fully characterized and their solid-state structures have been studied by means of single-crystal X-ray diffraction analysis. Nine of the 13 complexes carry reactive alkyl, amide or hydride groups, which indicates their potential as catalysts or supports for (transition) metals.

Introduction

Ligands possessing two binding sites play a pivotal role in modern coordination chemistry as they grant access to mono-, di- and polynuclear species from all sections of the periodic table.[1] As multidentate chelates, they give rise to stable mononuclear metal complexes and allow controlling the steric constraints with respect to both, shielding of the metal centre and adjusting the stereochemical properties of the thus formed complex. Furthermore, these ditopic ligands also offer the advantage of bringing two and sometimes more metal centres in close proximity. With respect to catalysis, dinuclear complexes allow cooperative or synergistic effects to arise[2] and framing two metals within a single molecule avoids ill-defined monomer/dimer equilibria. Hence, such complexes regularly excel their mononuclear counterparts in terms of reactivity and selectivity and allow achieving reactions that are not accessible with complexes possessing only one metal centre. In this regard, selecting appropriate ligands is crucial and even small changes with respect to electronic and/or steric implications may have a significant impact on the coordination behaviour. In main-group chemistry, which attracted much interest within the last decades,[3] two ligand classes received particular attention: bis(N-heterocyclic carbene)s[4] and *N*,*N*-dinucleating ligands.[1h] With respect to the latter, bis(amidine)s (**A**)[5] have been frequently used and noticeable effort has been directed towards bis(guanidine)s (**B**)[6] and bis(β-diketimine)s (**C**),[7] Fig. 1. However, the redox activity and non-innocence is well document for β-diketimines[8] and related ligands and ligand-centered side reactions have also been reported for bis(β-diketiminate) complexes.[7r] The saturated backbone of *N*,*N*′,*N*′-substituted 1,2-ethanediamines (**D**) prevents conjugation and hence delocalization,[9] which makes the related bis(*N*,*N*′,*N*′-substituted 1,2-ethanediamine)s interesting targets for ligand design. Due to the asymmetric nature of *N*,*N*′,*N*′-substituted 1,2-ethanediamines, bridging is either achieved through the secondary or tertiary amine groups giving rise to protio-ligands of type **1** and **2**, respectively, Fig. 1.

In 2003, the group of Hagadorn reported about the first example of a type **1** bis(*N*,*N*′,*N*′-substituted 1,2-ethanediamine) containing a dibenzofuran-bridge.[10] Notably, the authors defined the new ligand class as bis(amidoamine)s and as this notation has been adopted in the literature, we will also make

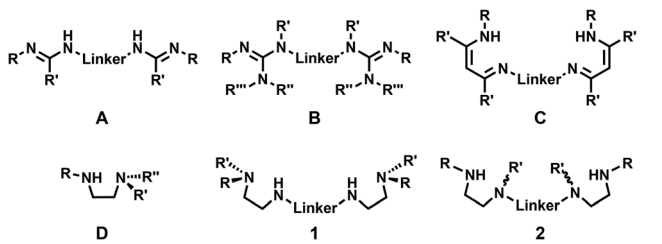

Fig. 1 Bis(amidine)s (**A**), bis(guanidine)s (**B**), bis(β-diketimine)s (**C**), *N*,*N*′,*N*′-substituted 1,2-ethanediamines (**D**), and bis(amidoamine)s of type **1** and **2** reported herein.

[a]*Institute of Inorganic Chemistry, University of Regensburg, Universitätsstraße 31, 93053 Regensburg, Germany*
[b]*Institute of Inorganic and Analytical Chemistry (IAAC), Friedrich Schiller University Jena, Humboldtstraße 8, 07743 Jena, Germany*
[c]*Jena Center for Soft Matter (JCSM), Friedrich Schiller University Jena Philosophenweg 7, 07743 Jena, Germany. E-mail: robert.kretschmer@uni-jena.de*

†Electronic supplementary information (ESI) available: Experimental details concerning the ligand synthesis, crystallographic data and NMR as well as IR spectra. CCDC 2026430–2026444. For ESI and crystallographic data in CIF or other electronic format see DOI: 10.1039/d0dt03124k

use of it in the following. Although, the related dinuclear metal complexes showed remarkable reactivity and catalytic activity,[10,11] no further investigations with respect to the ligand itself have been reported. However, its non-innocence in terms of hydride abstraction from a methylene group by forming a C=N double bond was observed when treating dinuclear zinc enolate complexes with tris(pentafluorophenyl) borane.[11c] As such a kind of reactivity was previously observed for *N*,*N*-alkylated anilines,[12] this behavior might be due to the aromatic linker group and could be avoided by using alternative bridging units. In addition, type **2** bis(amidoamine)s have no precedence in the literature. Hence, we set out to synthesize new bis(amidoamine)s of type **1** and **2** and investigated their reactivity towards aluminium, magnesium, tin, and zinc precursors. Our findings are reported herein.

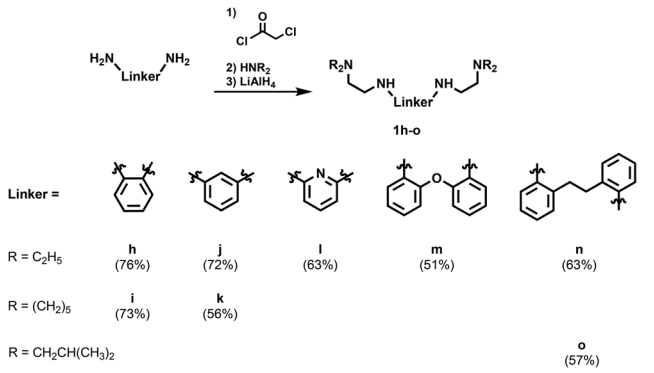

Scheme 2 Synthesis of bis(amidoamine)s of type **1** from primary diamines.

Results and discussion

Protio-ligand synthesis

The only yet reported dibenzofuran-bridged type **1** bis(amidoamine)s have been synthesized by the copper-catalyzed coupling of 4,6-diiodibenzofurane and alkylated ethylenediamines.[10,11a] As this approach is limited to aromatic linker groups, we established alternative synthetic protocols towards the bis(amidoamine)s **1** and **2**, respectively, which will be discussed consecutively in the following.[13]

With respect to type **1** bis(amidoamine)s possessing terminal tertiary and lateral secondary amine functions, two general approaches have been applied, Schemes 1 and 2. The first one originates from *N*,*N*-substituted ethylene diamines and a dicarbonyl precursor, *i.e.*, diethyl oxalate, dimethyl succinate and isophthalaldehyde. The thus formed amides and imines were subsequently reduced using $LiAlH_4$ and $NaBH_4$, respectively, affording the ethylene, butylene, and 1,3-xylylene bridged bis(amidoamine)s **1a–g** in yields ranging from 41 to 88%. The second approach starts from aromatic diamines that are converted first to the respective bis(α-haloamide)s by using chloro acetylchloride. Nucleophilic substitution of the halide with aliphatic secondary amines and reduction using lithium aluminium hydride allowed to isolate the bis(amidoamine)s **1h–o** in yields between 51 and 76%.

Bis(amidoamine)s of type **2**, which are bridged through the tertiary instead of the secondary amine, are also synthesized *via* two routes, Scheme 3. The piperazine-bridged compound **2a** is obtained in 52% yield by reacting piperazine with an α-chloroanilide and subsequent reduction using $LiAlH_4$. The acyclic species **2b–g**, however, were alternatively synthesized from *N*-methyl-*N*′-aryl substituted ethylenediamines and a suitable dihalide and obtained in yields ranging from 21 to 99%.

The ^{1}H NMR spectra of the protio-ligands in $CDCl_3$ have the expected pattern characteristic for a symmetric or averaged structure in solution. In order to elucidate the situation in the solid state, single-crystals of **2a** and **2b**, suitable for an X-ray diffraction analysis could be obtained. Their molecular structures are shown in Fig. 2. In brief, the piperazine unit within **2a** possesses the expected chair conformation and the two binding pockets occupy the equatorial positions while directing in opposite directions, a behaviour well known for other piperazine-bridged ligands.[14] In **2b**, the two binding pockets are also directed away from each other. Both species feature comparable N–C–C–N dihedral angles of 55.79(12) to 59.11(12)° as well as C–N bond lengths in between 1.4629(16) and 1.4682(16) Å, which are in good agreement with values of the related *N*,*N*′,*N*′-substituted 1,2-ethane-diamines (55.65(12)° and 1.4627(15)–1.4637(13) Å).[9a]

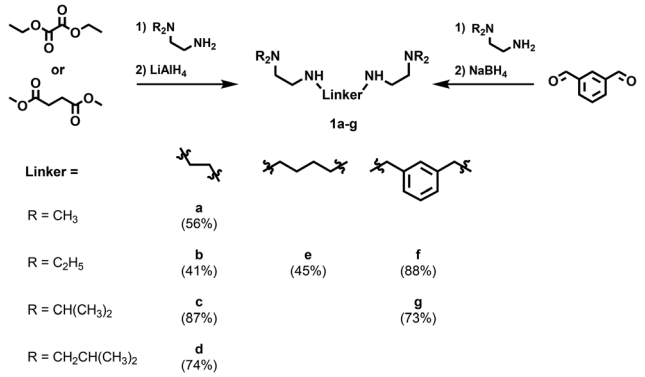

Scheme 1 Synthesis of bis(amidoamine)s of type **1** starting from dicarbonyl precursors.

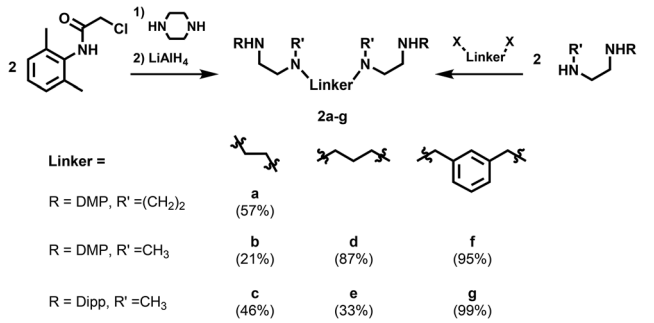

Scheme 3 Synthesis of bis(amidoamine)s of type **2**. DMP = 2,6-dimethylphenyl, Dipp = 2,6-diisopropylphenyl, X = Br, Cl.

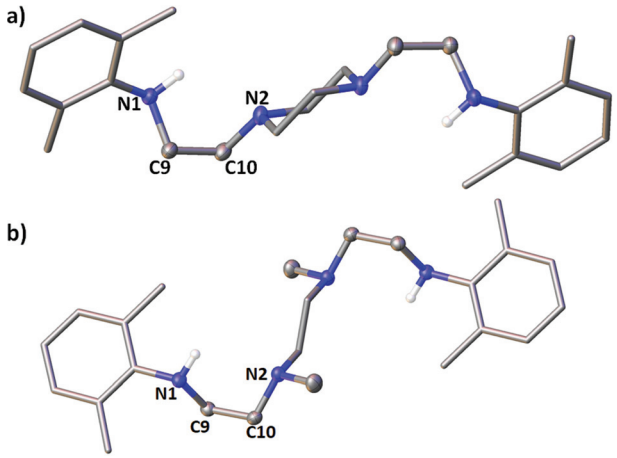

Fig. 2 Solid-state structures (hydrogen atoms except the NH are omitted for clarity) with selected bond lengths [Å]: (a) **2a**: N1–C9 1.4682 (16), C9–C10 1.5221(19), N2–C10 1.4629(16); (b) **2b**: N1–C9 1.4675(14), C9–C10 1.5188(12), N2–C10 1.4657(14).

Synthesis and structural characterization of mono- and dinuclear complexes

The stereochemistry of the mono- and dinuclear complexes originating from the protio-ligands of type **1** and **2** is significantly affected by the way both binding pockets are connected. Upon complexation, rapid inversion of the nitrogen atom of the tertiary amine is effectively cancelled out locking the overall configuration. In case of the protio-ligands **1a–n** this does not affect the overall stereochemistry of the thereby formed mono- and dinuclear complexes, Fig. 3. Complexation of the protio-ligands **2b–g**, however, gives rise to two chiral nitrogen-donor atoms and possibly induces the formation of several diastereomers.

While repeated attempts to obtain magnesium or zinc complexes starting from the protio-ligand **1m** remained unsuccessful, we were able to isolate well-defined compounds using **1n**, Scheme 4. In detail, **1nMg** was obtained by using magnesium bis[bis(trimethylsilyl)amide] while diethyl zinc was used to synthesize the respective zinc complex **1nZn**. Both complexes could be isolated as colourless crystals, which were suitable for

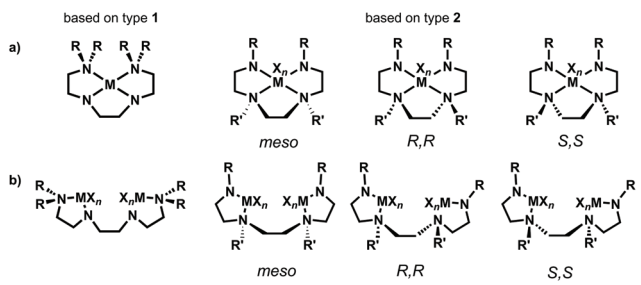

Fig. 3 Coordination modes of (a) mono- and (b) dinuclear complexes originating from the protio-ligands **1** and **2**, respectively. The ethylene-bridge was chosen as an example assuming R′ having the lowest Cahn–Ingold–Prelog-priority.

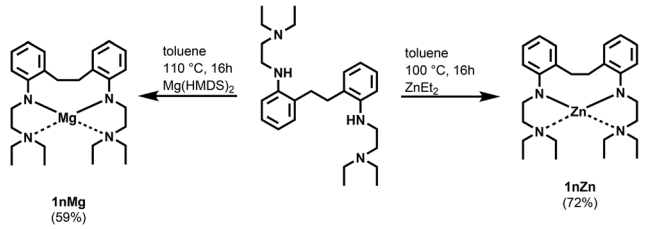

Scheme 4 Deprotonation of **1n** by magnesium bis[bis(trimethylsilyl) amide] or diethyl zinc.

X-ray diffraction (XRD) analyses and their molecular structures in the solid state are shown in Fig. 4; **1nZn** crystallizes as two independent molecules, which differ in their conformation, Fig. S1.† Within the homoleptic complexes **1nMg** and **1nZn**, the metal centre is four-fold-coordinated by the two *N*,*N*-chelates. As expected, the dative M–N1 and M–N4 bonds (Mg: 2.1679(14) and 2.1731(14) Å; Zn: 2.1685(12) and 2.1690(13) Å) are longer compared to the normal M–N2 and M–N3 bonds by about 0.16 (Mg) and 0.23 Å (Zn). Notably, only the normal bonds are significantly affected by the central atom, with shorter bond lengths in case of zinc (1.9383(13) and 1.9448(14) Å) as compared to magnesium (2.0071(15) and 2.0112(14) Å). The N–M–N bite angles, finally, remain by and large unaffected by the central metal, *i.e.*, 82.95(5) and 83.5(6)° in case of magnesium and 83.69(5) and 84.59(5)° for zinc. Notably, anagostic Mg···HC interactions (2.3324(5) and 2.3667(5) Å) with the methylene unit of the backbone are observed, while the contacts are significant longer in case of **1nZn** (2.4260(3) and 2.4391(4) Å).

The behaviour in solution differs for both complexes. In case of **1nMg**, a complex pattern of sharp resonances indicates a species of low symmetry. Notably, the number of resonances

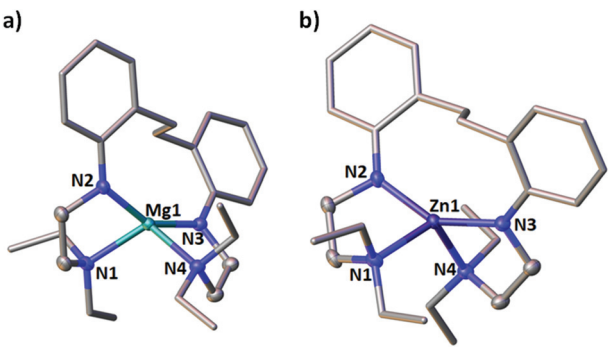

Fig. 4 Solid-state structures (hydrogen atoms except those of the anagostic bonds are omitted for clarity) with selected bond lengths [Å] and angles [°]: (a) **1nMg**: Mg1–N1 2.1679(14), Mg1–N2 2.0071(15), Mg1–N3 2.0112(14), Mg1–N4 2.1731(14), N1–Mg1–N2 83.55(6), N1–Mg1–N3 115.0866(8), N1–Mg1–N4 111.1091(7), N2–Mg1–N3 148.36256(7), N2–Mg1–N4 115.3234(9), N3–Mg1–N4 82.95(5); (b) **1nZn**: Zn1–N1 2.1685 (12), Zn1–N2 1.9448(14), Zn1–N3 1.9383(13), Zn1–N4 2.1690(13), N1–Zn1–N2 83.69(5), N1–Zn1–N3 116.3320(4), N1–Zn1–N4 110.8010(8), N2–Zn1–N3 146.9457(2), N2–Zn1–N4 113.9624(4), N3–Zn1–N4 84.59(5).

is strongly solvent-dependent and increases in going from THF-d_8 to C_6D_6. In the former case, one triplet and one quartet account for the terminal ethyl substituents, while they are split into two triplets and two quartets in C_6D_6 solution. The same holds true for the methylene groups of both, the ligands' backbone and the bridge which appear as three and six multiplets in THF-d_8 and in C_6D_6, respectively. **1nZn** was only soluble in a mixture of THF-d_8 and C_6D_6 and the ^{1}H NMR spectrum features broadened resonances for the ethyl groups, indicating slow conformational exchange at room temperature on the NMR time scale, while well-resolved signals were observed for the protons of both, the methylene units and the aromatic ring. The latter finding is consistent with a pseudo C_2-symmetric structure of the ligand framework in solution.

We next became interested if dinuclear aluminium(III) and tin(II) complexes are accessible starting from the protio-ligands **1**. Hence, **1j** and **1k** were allowed to react with aluminium hydride trimethylamine, while **1m** and **1n** were treated with tin bis[bis(trimethylsilyl)amide], Scheme 5. Please note that the reactions of **1a** and **1d** with Sn(HMDS)$_2$ yielded only a complex reaction mixture. The dinuclear aluminium(III) hydride complexes **1jAlH$_2$** and **1kAlH$_2$** were obtained in excellent yields of 92% and 99%, respectively. Although we could also isolate the dinuclear tin(II) complexes **1mSnHMDS** and **1nSnHMDS**, the yields were significantly lower (14 and 41%, respectively). As all four compounds were isolated as crystalline material, an XRD analysis allowed to derive their molecular solid-state structures, which are shown in Fig. 5 and 6. **1jAlH$_2$** and **1kAlH$_2$** feature two tetra-coordinated aluminium centres that are facing away from eachother. The Al1–N1 and Al1–N2 bond lengths of both compounds are comparable and resemble values of aluminium complexes of *N*,*N*′,*N*′-substituted 1,2-ethanediamine ligands.[9a] The Al–H bond lengths (1.516(15)–1.56(2) Å) and H–Al–H bond angles (109.6(12) and 119.5(11)°) are reminiscent of values reported before for mononuclear aluminium dihydride complexes based on *N*,*N*-chelating ligands (1.379(45)–1.611(19) Å; 109.4(16)–122(2)°).[15] The room temperature ^{1}H NMR spectra **1jAlH$_2$** and **1kAlH$_2$** in $CDCl_3$ are distinctly different: in the first case, a simple set of resonances, *i.e.* one triplet and quartet representing the terminal ethyl rests but also the expected singlet : doublet : triplet pattern of the aryl-bridge, account for a symmetric or averaged structure in solution. In case of **1kAlH$_2$**, however, a series of sharp multiplets including the resonances of the 1,3-phenylene-bridge indicate the presence of at least two conformers that do not undergo rapid exchange. The presence of an AlH_2 group was established by ^{1}H NMR spectroscopy and the AlH_2 resonances appear as broad singlets at 3.90 and 3.97 ppm, respectively. Further evidence is given by the asymmetric and symmetric Al–H stretches that occur at 1780 and 1808 cm^{-1} as well as 1775 and 1805 cm^{-1}. The mean values, *i.e.*, 1794 and 1790 cm^{-1}, are significantly red-shifted compared to aluminium hydrides based on other *N*,*N*-chelating ligands.[6i,16]

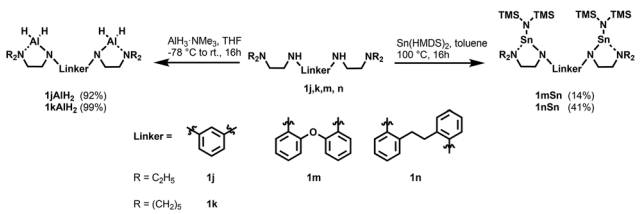

Scheme 5 Synthesis of dinuclear aluminium(III) and tin(II) complexes.

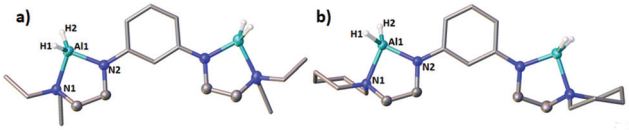

Fig. 5 Solid-state structures (hydrogen atoms except the AlH and cocrystallized THF in case of **1kAlH$_2$** are omitted for clarity) with selected bond lengths [Å] and angles [°]: (a) **1jAlH$_2$**: Al1–N1 1.9972(12), Al1–N2 1.8479(15), Al1–H1 1.54 (2), Al1–H2 1.516(15), N1–Al1–N2 87.40 (5), H1–Al1–H2 119.5(11); (b) **1kAlH$_2$**: Al1–N1 2.0042(14), Al1–N2 1.8473 (14), Al1–H1 1.56(2), Al1–H2 1.54(2), N1–Al1–N2 88.80(6), H1–Al1–H2 113.7(12).

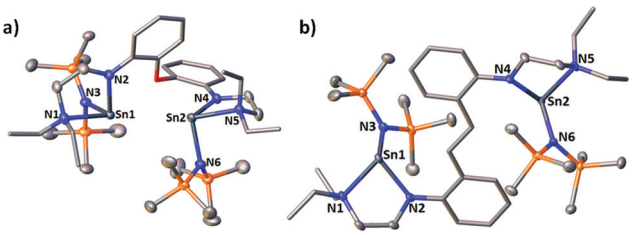

Fig. 6 Solid-state structures (hydrogen atoms are omitted for clarity) with selected bond lengths [Å] and angles [°]: (a) **1mSnHMDS**: Sn1–N1 2.453(3), Sn1–N2 2.139(2), Sn1–N3 2.154(3), Sn2–N4 2.165(2), Sn2–N5 2.374(3), Sn2–N6 2.165(3), N1–Sn1–N2 75.58(9), N4–Sn2–N5 76.07(9); (b) **1nSnHMDS**: Sn1–N1 2.3904(18), Sn1–N2 2.1690(18), Sn1–N3 2.1520 (17), Sn2–N4 2.1513(16), Sn2–N5 2.3666(17), Sn2–N6 2.1440(17), N1–Sn1–N2 79.27(6), N4–Sn2–N5 78.32(6).

Within the distannylenes **1mSnHMDS** and **1nSnHMDS** the tin(II) centres are surrounded by an overall pyramidal ligand array and reside in a distorted tetrahedral environment with one vertex occupied by a stereo-chemically active lone pair of electrons, Fig. 6. The Sn–N(TMS)$_2$ bond lengths (2.1440(17)–2.165(3) Å) are in good agreement with those reported of related mono- (2.109(4)–2.150(2) Å)[17] and distannylenes (2.124(2)–2.140(5) Å)[18] involving *N*,*N*-chelating ligands. The room temperature ^{1}H NMR spectrum of **1mSnHMDS** in toluene-d_8 consists of a series of broad resonances that eventually collapse upon heating to 353 K to well-defined signals being in agreement with a symmetric or averaged structure in solution. This indicates hindered motion of the molecule likely due to the more rigid oxydiphenylene-bridge. In contrast, the resonance sets of **1nSnHMDS** in C_6D_6 are symmetrical due to conformational averaging on the NMR time scale illustrating the increased flexibility of the bridging group.

After having studied the coordination behaviour of the protio-ligands **1**, we became interested in the complexation abilities of **2**. As discussed above, the coordination of the

lateral tertiary nitrogen atoms induces chirality and possibly leads to various diastereomers, Fig. 3. **2a** possesses a bridging piperazine ring and the two lateral nitrogen atoms do not become chiral upon complexation. However, two isomers, *i.e.*, *anti* and *syn*, are conceivable when assuming a chair conformation of the central piperazine ring.

Reacting **2a** with trimethylaluminium or diethyl zinc affords the complexes **2aAlMe$_2$** and **2aZnEt** in 81% and 21% yield, respectively, as colourless crystals, Scheme 6. Their molecular structures in the solid state are given in Fig. 7 and as expected, both complexes exist in the *anti*-configuration, *i.e.*, both binding sites are directed in opposite directions. The structural parameters including the Al–N (1.8361(13) and 2.0723(13) Å) and Al–C (1.9680(17)–1.9722(16) Å) bond lengths of **2aAlMe$_2$** are comparable to those of the related mononuclear counterpart.[9a] While for **2aZnEt** no related mononuclear relative has so far been reported, the Zn–C bond lengths (1.958(2)–1.972(2) Å) are in good agreement with values reported for comparable mononuclear complexes based on *N,N*-chelating ligands (1.964(5)–2.002(2) Å).[19]

In going from **2a** to the more flexible protio-ligand **2b**, the reaction with diethyl zinc does not afford a heteroleptic dinuclear complex but instead the mononuclear homoleptic complex **2bZn** is formed in 82% yield, Scheme 7. As expected, the same holds true for the reaction of **2b** with magnesium bis[bis(trimethylsilyl)amide], which gives rise to **2bMg** (65% yield). Single crystals of both compounds could be obtained

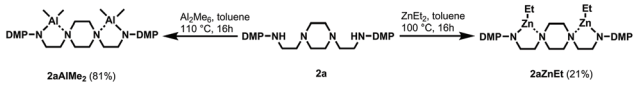

Scheme 6 Synthesis of dinuclear aluminium(III) and zinc(II) complexes starting from **2a**.

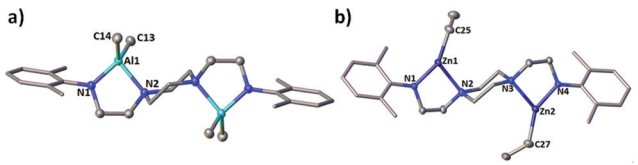

Fig. 7 Solid-state structures (hydrogen atoms are omitted for clarity) with selected bond lengths [Å] and angles [°]: (a) **2aAlMe$_2$**: Al1–N1 1.8361(13), Al1–N2 2.0723(13), Al1–C13 1.9722(16), Al1–C14 1.9680(17), N1–Al1–N2 87.35(5), C13–Al1–C14 113.28(7); (b) **2aZnEt**: Zn1–N1 1.8920(17), Zn1–N2 2.2060(12), Zn1–C25 1.972(2), Zn2–N3 2.1842(12), Zn2–N4 1.8966(17), Zn2–C27 1.958(2), N1–Zn1–N2 85.33(6), N3–Zn2–N4 85.27(6).

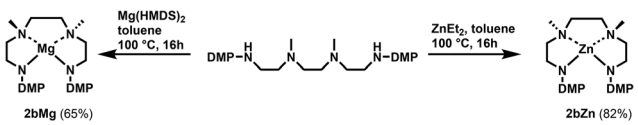

Scheme 7 Synthesis of homoleptic magnesium and zinc complexes starting from **2b**.

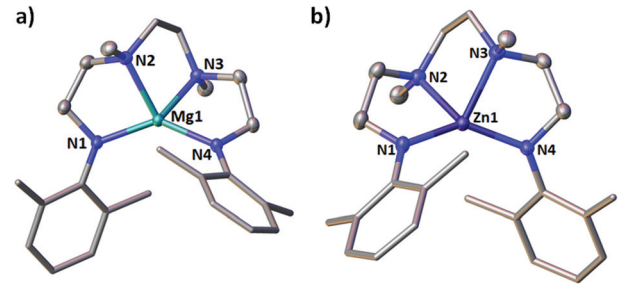

Fig. 8 Solid-state structures (hydrogen atoms are omitted for clarity) with selected bond lengths [Å] and angles [°]: (a) **2bMg**: Mg1–N1 2.0027(9), Mg1–N2 2.1781(10), Mg1–N3 2.1968(10), Mg1–N4 2.0009(8), N1–Mg1–N2 85.42(4), N3–Mg1–N4 85.89(4); (b) **2bZn**: Zn1–N1 1.9291 (13), Zn1–N2 2.1882(12), Zn1–N3 2.2091(11), Zn1–N4 1.9281(13), N1–Zn1–N2 85.81(5), N3–Zn1–N4 86.49(5).

and their molecular structures have been investigated by an XRD analysis, Fig. 8.

2bMg and **2bZn** crystallize in the centrosymmetric space groups $P2_1/c$ and $P2_1/n$, respectively, and accommodate hence equal numbers of the *R,R*- and *S,S*-diastereomers. While the obtained molecular structures do not allow deducing information of the bulk sample, ^{1}H NMR spectroscopic data (measured in THF-d$_8$ and in C$_6$D$_6$/THF-d$_8$, respectively) give no evidence for the presence of the *meso*-diastereomer. Characteristic features are two singlets integrating for 12 and 6 protons, respectively, accounting for the methyl groups at the 2,6-DMP substituent and at the lateral nitrogen atoms. The latter resonance is significantly affected by the central metal and appears at 2.59 ppm in case of magnesium while it is shifted to higher field in case of zinc (2.14 ppm). The methylene resonances of the formed macrocycle split into several multiplets indicating separate signals for the axial and equatorial protons. Furthermore and due to anisotropic effects, the axial protons show smaller chemical shift values compared to their equatorial counterparts. The Mg–N and Zn–N bond lengths with values of 2.0009(8) to 2.1968(10) Å and 1.9281(13) to 2.2091(11) Å, respectively, as well as the N–M–N bite angles (85.42(4) and 85.89(4)° (Mg) and 85.81(5) and 86.49(5)° (Zn)) resemble those of the mononuclear complexes **1nMg** and **1nZn** discussed before. However, the shorter ethylene-bridge in case of **2bMg** and **2bZn** induces wider NMN plane to plane twist angles (118.73(4) and 118.12(4)°, respectively) as compared to the related complexes of **1n** (99.17(6) and 98.75(5)° for **1nMg** and **1nZn**, respectively).

Reacting the protio-ligand **2b** with aluminium hydride trimethylamine yields the mononuclear complex **2bAlH**, regardless of whether one or two equivalents of AlH$_3$·NMe$_3$ were used, Scheme 8. Its molecular solid-state structure has been

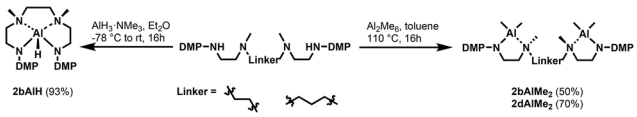

Scheme 8 Synthesis of mono- and dinuclear aluminium complexes.

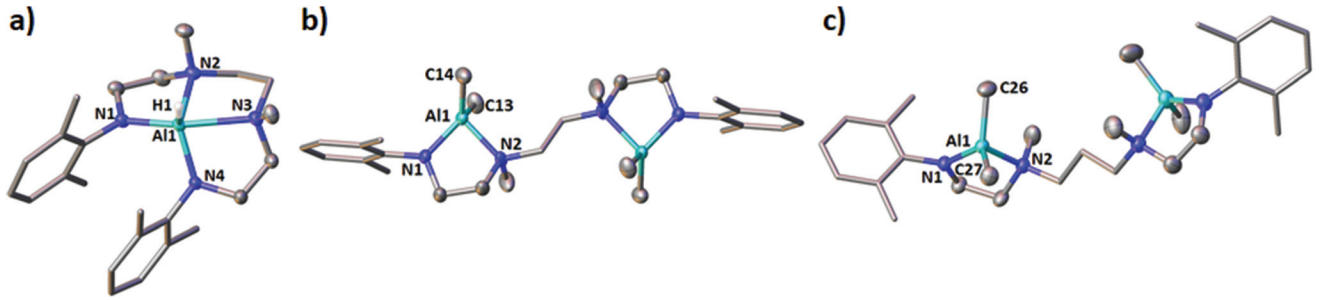

Fig. 9 Solid-state structures (hydrogen atoms except the AlH and in case of **2bAlMe$_2$** a second independent molecule are omitted for clarity) with selected bond lengths [Å] and angles [°]: (a) **2bAlH**: Al1–N1 1.8924(13), Al1–N2 2.0771(11), Al1–N3 2.3482(13), Al1–N4 1.8520(11), Al1–H1 1.522(17), N1–Al1–N2 83.17(5), N3–Al1–N4 79.31(5); (b) **2bAlMe$_2$**: Al1–N1 1.8324(16), Al1–N2 2.021(10), Al1–C13 1.984(6), Al1–C14 1.939(8), N1–Al1–N2 87.0 (2), C13–Al1–C14 114.7(3); (c) **2dAlMe$_2$**: Al1–N1 1.8352(14), Al1–N2 2.0400(16), Al1–C26 1.975(2), Al1–C27 1.9759(19), N1–Al1–N2 87.21(6), C26–Al1–C27 114.09(9).

analysed by single-crystal XRD revealing the presence of the *meso*-diastereomer and the two NCH_3 groups and the hydride ligand are oriented in the same direction, Fig. 9a. The ^{1}H NMR spectrum recorded in C_6D_6 shows two singlets for the DMP methyl groups indicating hindered rotation about the N–C_{aryl} bond. One singlet accounts for the methyl groups bound to the lateral nitrogen atoms while the resonances of the linkers' methylene groups appear a several multiplets in agreement with a locked conformation of the macrocycle. The Al–N bonds (1.8520(11) to 2.3482(13) Å) are in the range of the dinuclear complexes **1jAlH$_2$** and **1kAlH$_2$** discussed above. The Al–H bond length (1.522(17) Å) is in good agreement with values reported before for other aluminium(III) monohydride complexes involving four Al–N bonds (1.48(4) to 1.607(15) Å).[20] The Al–H stretching frequency of 1735 cm^{-1} falls well in between previously reported values of 1693 to 1836 cm^{-1}.[20b,d,21]

Changing the aluminium source to trimethyl aluminium does not afford the respective mononuclear complex but instead the dinuclear aluminium alkyl complex **2bAlMe$_2$** is formed in 50% yield. The same holds true for the propylene-bridged protio-ligand **2d**, which affords the dinuclear complex **2dAlMe$_2$** in 70% yield. Their molecular structures in the solid state are shown in Fig. 9. In case of **2bAlMe$_2$**, the *meso*-diastereomer was observed by XRD, while in case of **2dAlMe$_2$** the *S*,*S*-diastereomer was detected, but the centrosymmetric $P2_1/c$ space group indicates that **2dAlMe$_2$** is obtained as a mixture of enantiomers. Please note, that increasing the lengths of the linker group changes the priorities according to the Cahn–Ingold–Prelog priority rules although **2bAlMe$_2$** and **2dAlMe$_2$** are virtually identical.[22] Both species possess two tetra-coordinated aluminium centres. The Al–C and Al–N bond lengths (1.939(8)–1.984(6) Å and 1.8302(14)–2.0400(16) Å, respectively) as well as the C–Al–C and N–Al–N bond angles (113.08(13)–114.7(3)° and 87.0(2)–87.21(6)°, respectively) are in good agreement with those of **2aAlMe$_2$** and the related mononuclear congeners.[9a] The ^{1}H NMR spectrum of **2bAlMe$_2$** recorded in $CDCl_3$ contains two sets of four and two partially overlapping singlets that were assigned to the respective Al(CH_3) and N(CH_3) groups and indicate a mixture of the *meso*- and *R*,*R*/*S*,*S*-diastereomers. In case of **2dAlMe$_2$**, the unsymmetrical substitution pattern at aluminium gives rises to two singlets accounting for the two Al(CH_3) groups and the N(CH_3) groups appear as one singlet. Notably, the longer propylene-bridge in case of **2dAlMe$_2$** might causes the equivalence of the proton resonances of the *meso*- and *R*,*R*/*S*,*S*-diastereomers. In both complexes, free rotation about the N–C_{aryl} bond is evidenced by a simples set of resonances of the DMP group, *i.e.*, one singlet, one doublet, and one triplet integrating for 12, 4 and 2 protons, respectively.

Conclusions

In summary, we report about the synthesis of two general types of bis(amidoamine) ligands, in which the tertiary amine functions reside either on the lateral (type **2**) or terminal (type **1**) positions. Five synthetic procedures starting from readily available precursors have been employed and allowed for the gram-scale synthesis of the protio-ligands with yields ranging from 21 to 99%. Starting from the protio-ligands of type **1**, we could successfully isolate and fully characterize six complexes. Due to the flexibility of bridging groups, the reactions incorporating Mg(HMDS)$_2$ or $ZnEt_2$ afforded the mononuclear homoleptic complexes **1nMg** and **1nZn**, respectively, in-line with a Schlenk equilibrium. In contrast, originating from AlH_3·NMe_3 and Sn(HMDS)$_2$ gave rise to the dinuclear complexes **1jAlH$_2$**, **1kAlH$_2$**, **1mSnHMDS**, and **1nSnHMDS**. The presence of reactive amide and hydride functions in the dinuclear complexes indicates possible applications, *i.e.*, as ligands for (transition) metals or as catalysts in their own rights. Using the piperazine-bridged ligand **2a**, dinuclear Janus-type complexes of aluminium and zinc could be obtained. The flexible ethylene-bridged ligand **2b** shows a variety of coordination modes upon complexation and the pro-chirality of the lateral tertiary amine groups affects the overall geometry of the obtained products. Mononuclear complexes of aluminium, magnesium, and tin were isolated after the reaction with AlH_3·NMe_3, Mg(HMDS)$_2$, and $ZnEt_2$, respectively, while dinuclear complexes were derived from **2b** and trimethyl aluminium. The related species crystallize in centrosymmetric space groups and

different diastereomers were identified from their molecular solid-state structures. The *R*,*R* or *S*,*S* form was observed in case of **2bMg**, **2bZn**, **2dAlMe$_2$**, while the *meso* form was observed for **2bAlH** and **2bAlMe$_2$**. In solution, however, a second set of resonances in the ^{1}H NMR spectrum indicates a mixture of the *meso* and the *R*,*R*/*S*,*S*-diastereomers for **2bAlMe$_2$**, while the spectra of **2bAlH**, **2bMg**, **2bZn**, and **2dAlMe$_2$** shown only one set of resonances. The catalytic activity of the heteroleptic complexes and their coordination capabilities towards transition metals will be further investigated in the future.

Experimental section

General considerations

All preparations were performed under an inert atmosphere of dinitrogen by means of standard Schlenk-line techniques, while the samples for analytics were handled in a glovebox (MBraun). Yields are nonoptimized and refer to isolated crystalline material. All solvents (toluene, *n*-pentane, *n*-hexane, tetrahydrofuran) were distilled from Na/benzophenone prior to use while C_6D_6, THF-d_8 and toluene-d_8 were dried using molecular sieves (4 Å).

1nMg: Mg(HMDS)$_2$ (485 mg, 1.40 mmol) was added to a stirred solution of **1n** (275 mg, 0.67 mmol) in toluene (8 mL) and stirred at 110 °C overnight resulting in a pale brown solution. After cooling to room temperature the solvent was removed and the brown solid was washed with *n*-pentane (1 × 10 mL). The solid was dissolved in THF (5 mL), filtered off and a few drops of *n*-pentane were added to the solution. After standing at room temperature overnight, **1nMg** (171 mg, 0.40 mmol, 59%) could be isolated as clear colourless crystals.

^{1}H NMR (400 MHz, C_6D_6): δ (ppm) = 7.49 (t, J = 7.5 Hz, 2H, C_6H_4), 7.28 (d, J = 7.3 Hz, 2H, C_6H_4), 6.78–6.75 (m, 4H, C_6H_4), 3.55–3.47 (m, 2H, $C_6H_4CH_2CH_2C_6H_4$), 3.34–3.30 (m, 2H, $NCH_2CH_2NC_6H_4$), 3.04–2.96 (m, 2H, $NCH_2CH_2NC_6H_4$), 2.86–2.77 (m, 2H, $C_6H_4CH_2CH_2C_6H_4$), 2.43–2.15 (m, 10H, $NCH_2CH_2NC_6H_4$ + NCH_2CH_3), 2.06–1.97 (m, 2H, $NCH_2CH_2NC_6H_4$), 0.51 (t, J = 7.2 Hz, 6H, NCH_2CH_3), 0.38 (t, J = 7.2 Hz, 6H, NCH_2CH_3); ^{1}H NMR (400 MHz, THF-d_8): δ (ppm) = 6.87 (dt, J = 8.0 Hz, 2H, C_6H_4), 6.79 (dd, J = 7.1 Hz, 2H, C_6H_4), 6.28 (d, J = 8.0 Hz, 2H, C_6H_4), 6.16 (dt, J = 7.2 Hz, 2H, C_6H_4), 3.41–3.28 (m, 4H, $C_6H_4CH_2CH_2C_6H_4$ + $NCH_2CH_2NC_6H_4$), 3.13–2.97 (m, 6H, $NCH_2CH_2NC_6H_4$), 2.87 (q, 8H, J = 7.1 Hz, NCH_2CH_3), 2.40–2.30 (m, 2H, $C_6H_4CH_2CH_2C_6H_4$), 1.03 (t, J = 8.3 Hz, 12H, NCH_2CH_3); ^{13}C{H} NMR (101 MHz, C_6D_6): δ (ppm) = 156.6 (C_6H_4), 130.4 (C_6H_4), 128.7 (C_6H_4), 126.8 (C_6H_4), 112.5 (C_6H_4), 110.7 (C_6H_4), 52.7 ($C_6H_4CH_2CH_2C_6H_4$), 45.0 (NCH_2CH_2N), 45.0 (NCH_2CH_2N), 39.2 (NCH_2CH_3), 33.8 (NCH_2CH_3), 8.6 (NCH_2CH_3), 8.5 (NCH_2CH_3); IR (ATR): $\tilde{\nu}$ [cm^{-1}] = 3048 (w), 2966 (w), 2925 (w), 2865 (w), 2795 (w), 1590 (m), 1486 (m), 1440 (m), 1304 (s), 1155 (m), 1083 (m), 746 (s), 728 (vs); anal. calc. (found) for [$C_{26}H_{40}MgN_4$]: C 72.13 (72.23), H 9.31 (8.91), N 12.94 (12.75).

1nZn: Zn(Et)$_2$ (1.20 mL, 1.20 mmol, 1.0 M in hexanes) was added to a stirred solution of **1n** (235 mg, 0.57 mmol) in toluene (8 mL) and stirred at 100 °C overnight resulting in a yellow suspension. After cooling to room temperature the solids were filtered off and the filtrate concentrated to 5 mL. After standing at room temperature overnight, **1nZn** (195 mg, 0.41 mmol, 72%) was isolated as clear colourless crystals.

^{1}H NMR (400 MHz, C_6D_6 + THF-d_8): δ (ppm) = 7.25 (t, J = 7.5 Hz, 2H, C_6H_4), 7.08 (d, J = 7.1 Hz, 2H, C_6H_4), 6.64 (d, J = 8.2 Hz, 2H, C_6H_4), 6.55 (t, J = 7.2 Hz, 2H, C_6H_4), 3.96–3.89 (m, 2H, $C_6H_4CH_2CH_2C_6H_4$), 3.42–3.37 (m, 2H, $NCH_2CH_2NC_6H_4$), 3.06–2.98 (m, 2H, $NCH_2CH_2NC_6H_4$), 2.56–2.24 (m, 14H, $C_6H_4CH_2CH_2C_6H_4$ + $NCH_2CH_2NC_6H_4$ + NCH_2CH_3), 0.57 (br, 12H, NCH_2CH_3); ^{13}C{H} NMR (101 MHz, C_6D_6 + THF-d_8): δ (ppm) = 154.8 (C_6H_4), 130.5 (C_6H_4), 128.1 (C_6H_4), 126.6 (C_6H_4), 112.8 (C_6H_4), 111.8 (C_6H_4), 53.1 ($C_6H_4CH_2CH_2NC_6H_4$), 47.2 (NCH_2CH_3), 46.0 (NCH_2CH_2N), 40.9 (NCH_2CH_3), 33.5 (NCH_2CH_2N), 8.1 ($ZnCH_2CH_3$), 6.5 ($ZnCH_2CH_3$); IR (ATR): $\tilde{\nu}$ [cm^{-1}] = 3039 (w), 2931 (w), 2867 (w), 2799 (w), 1588 (m), 1473 (m), 1439 (m), 1306 (vs), 1085 (m), 924 (m), 745 (vs), 726 (vs); anal. calc. (found) for [$C_{26}H_{40}ZnN_4$]: C 65.88 (65.88), H 8.51 (8.40), N 11.82 (11.70).

1jAlH$_2$: A solution of **1j** (1.84 g, 6.00 mmol) in THF (60 mL) was cooled to −78 °C before it was added to AlH_3·NMe_3 (1.13 g, 12.6 mmol) followed by stirring at room temperature for 15 hours. The solvent was removed and the resulting solid was dried in vacuum to obtain **1jAlH$_2$** (2.00 g, 0.55 mmol, 92%) as a white powder. Crystals suitable for an XRD analysis were obtained from a saturated THF solution upon standing at room temperature.

^{1}H NMR (400 MHz, $CDCl_3$): δ (ppm) = 6.92 (t, J = 7.9 Hz, 1H, C_6H_4), 5.90 (dd, J = 7.9; 2.1 Hz, 2H, C_6H_4), 5.77 (s, 1H), 3.90 (br, 4H, AlH_2), 3.21 (t, J = 5.8 Hz, 4H, NCH_2CH_2N), 3.07–2.95 (m, 8H, NCH_2CH_3), 2.91–2.79 (m, 4H, NCH_2CH_2N), 1.17 (t, J = 7.2 Hz, 12H, NCH_2CH_3); ^{13}C{^{1}H} NMR (101 MHz, $CDCl_3$): δ (ppm) = 153.9 (C_6H_4), 129.4 (C_6H_4), 101.9 (C_6H_4), 98.02 (C_6H_4), 53.0 (CH_2CH_2), 43.9 (CH_2CH_2), 42.1 (CH_3CH_2), 8.5 (CH_3CH_2); IR (ATR): $\tilde{\nu}$ [cm^{-1}] = 2967 (w), 2924 (w), 2866 (w), 2804 (w), 1808 (m), 1780 (m), 1579 (m), 1466 (m), 1353 (m), 1264 (m), 1014 (m), 778 (s), 658 (vs), 535 (vs); anal. calc. (found) for [$C_{18}H_{36}N_4Al_2$·0.15 THF]: C 60.39 (60.73), H 10.14 (10.50), N 13.81 (14.13).

1kAlH$_2$: A solution of **1k** (330 mg, 1.00 mmol) in THF (15 mL) was cooled to −78 °C before it was added to AlH_3·NMe_3 (180 mg, 2.00 mmol) followed by stirring at room temperature for 1 hour. Upon standing at room temperature crystals of **1kAlH$_2$** (382 mg, 0.99 mmol, 99%) formed, which were collected and dried in vacuum.

^{1}H NMR (400 MHz, $CDCl_3$): δ (ppm) = 6.98–6.91 (m, 1H, C_6H_4), 6.00–5.90 (m, 2H, C_6H_4), 5.88–5.80 (m, 1H, C_6H_4), 3.97 (br, 4H, AlH_2), 3.36–3.25 (m, 8H, α-pip + $C_6H_4NCH_2CH_2$), 3.01 (t, J = 6.0 Hz, 4H, $C_6H_4NCH_2CH_2$), 2.34 (dt, J = 11.9 Hz, J = 2.6 Hz, 4H, α-pip), 2.02–1.74 (m, 8H, β-pip), 1.47–1.25 (m, 4H, γ-pip); ^{13}C{^{1}H} NMR (101 MHz, $CDCl_3$): δ (ppm) = 153.9 (C_6H_4), 129.7 (C_6H_4), 102.1 (C_6H_4), 98.3 (C_6H_4), 59.8 ($C_6H_4NCH_2CH_2$), 54.8 (α-pip), 41.7 ($C_6H_4NCH_2CH_2$), 24.2 (β-pip), 23.4 (γ-pip); IR (ATR): $\tilde{\nu}$ [cm^{-1}] = 2942 (w), 2856 (w), 1805 (w), 1775 (w), 1590 (m), 1469 (m), 1339 (m), 1229 (m),

1029 (m), 777 (s), 674 (vs); despite repeated attempts no suitable elemental analysis could be obtained.

1mSnHMDS: $Sn(HMDS)_2$ (706 mg, 0.62 mL, 1.61 mmol) was added to a stirred solution of **1m** (320 mg, 0.80 mmol) in toluene (8 mL) followed by stirring at 100 °C overnight resulting in a black solution. After cooling to room temperature the solvent was removed and *n*-pentane (5 mL) was added to the black oil resulting in the instant formation of crystals. After washing the crystals with *n*-pentane (3 × 2 mL), **1mSn** (110 mg, 0.12 mmol, 14%) could be isolated as slightly brownish crystals.

^{1}H NMR (400 MHz, 353 K, toluene-d_8): δ (ppm) = 7.22–7.20 (m, 1H, C_6H_4), 7.04–7.00 (m, 3H, C_6H_4), 6.68–6.64 (m, 2H, C_6H_4), 6.52–6.41 (m, 2H, C_6H_4), 3.37–3.23 (m, 4H, NCH_2CH_2N), 2.74–2.58 (m, 8H, NCH_2CH_2N + NCH_2CH_3), 2.51–2.42 (m, 4H, NCH_2CH_3), 0.89–0.79 (m, 12H, NCH_2CH_3), 0.26–0.22 (m, 36H, $SiCH_3$); $^{13}C\{^1H\}$ NMR: even after repeated attempts at various temperatures no suitable ^{13}C NMR spectrum could be obtained; IR (ATR): $\tilde{\nu}$ [cm^{-1}] = 3052 (vw), 2944 (w), 2894 (vw), 2865 (w), 2831 (w), 1594 (m), 1491 (s), 1305 (s), 1243 (s), 1126 (m), 930 (vs), 732 (vs), 662 (s); anal. calc. (found) for $[C_{36}H_{72}N_6OSi_4Sn_2]$: C 45.29 (45.46), H 7.60 (7.11), N 8.80 (8.69).

1nSnHMDS: $Sn(HMDS)_2$ (503 mg, 0.44 mL, 1.14 mmol) was added to a stirred solution of **1n** (235 mg, 0.57 mmol) in toluene (8 mL) followed by stirring at 100 °C overnight resulting in an orange solution and a grey precipitate. After cooling to room temperature the solids were filtered off and the filtrate was concentrated to dryness affording a dark orange solid. *n*-pentane (5 mL) was added causing the instant formation of **1nSn** (225 mg, 0.23 mmol, 41%) as an orange crystalline solid. Crystals suitable for an X-Ray diffraction analysis were obtained from recrystallization in a mixture of THF/*n*-pentane (1 : 1) at room temperature.

^{1}H NMR (400 MHz, C_6D_6): δ (ppm) = 7.55 (d, J = 6.1 Hz, 2H, C_6H_4), 7.36 (t, J = 7.4 Hz, 2H, C_6H_4), 6.96 (t, J = 6.9 Hz, 2H, C_6H_4), 6.89 (d, J = 8.1 Hz, 2H, C_6H_4), 3.64 (s, 4H, $C_6H_4CH_2CH_2C_6H_4$), 3.29–3.26 (m, 4H, NCH_2CH_2N), 2.48–2.45 (m, 12H, NCH_2CH_2N + NCH_2CH_3), 0.60 (t, J = 7.3 Hz, 12H, NCH_2CH_3), 0.36 (s, 36H, $SiCH_3$); $^{13}C\{^1H\}$ NMR (101 MHz, C_6D_6): δ (ppm) = 154.4 (C_6H_4), 130.0 (C_6H_4), 127.5 (C_6H_4), 116.7 (C_6H_4), 115.6 (C_6H_4), 54.0 ($C_6H_4CH_2CH_2C_6H_4$), 49.8 (NCH_2CH_2N), 43.9 (NCH_2CH_2N), 36.1 (NCH_2CH_3), 8.6 (NCH_2CH_3), 6.8 ($SiCH_3$); IR (ATR): $\tilde{\nu}$ [cm^{-1}] = 3057 (vw), 2945 (w), 2892 (vw), 2826 (w), 1591 (m), 1483 (m), 1438 (m), 1243 (s), 904 (vs), 821 (vs), 744 (s), 664 (s); anal. calc. (found) for $[C_{38}H_{76}N_6Si_4Sn_2{\cdot}0.15\ C_5H_{12}]$: C 47.61 (47.83), H 8.02 (7.67), N 8.60 (8.51).

2bMg: $Mg(HMDS)_2$ (1.57 g, 4.56 mmol) was added to a stirred solution of **2b** (830 mg, 2.17 mmol) in toluene (8 mL) and stirred at 100 °C overnight resulting in the formation of a white precipitate. After cooling to room temperature, the solids were filtered off and washed with *n*-pentane (3 × 5 mL) to obtain **2bMg** (570 mg, 1.40 mmol, 65%) as a white solid. Crystals suitable for an X-Ray diffraction analysis were obtained by extraction with hot THF (40 mL) followed by slow cooling to room temperature.

^{1}H NMR (400 MHz, THF-d_8): δ (ppm) = 6.66 (d, J = 7.3 Hz, 4H, m-C_6H_3), 6.22 (t, J = 7.2 Hz, 2H, p-C_6H_3), 3.09–2.92 (m, 6H, $NCH_2CH_2NC_6H_3$), 2.89–2.82 (m, 2H, NCH_2CH_2N), 2.59 (s, 6H, NCH_3) 2.57–2.53 (m, 2H, $NCH_2CH_2NC_6H_3$), 2.19 (s, 12H, $CH_3C_6H_3$); $^{13}C\{^1H\}$ NMR: due to the low solubility of the complex, even after extended scans no suitable ^{13}C NMR spectrum could be obtained; IR (ATR): $\tilde{\nu}$ [cm^{-1}] = 3045 (w), 2965 (w), 2804 (w), 2788 (w), 1588 (m), 1470 (m), 1415 (m), 1280 (m), 1074 (m), 760 (vs), 740 (s); anal. calc. (found) for $[C_{24}H_{36}MgN_4]$: C 71.20 (71.13), H 8.96 (8.63), N 13.84 (13.72).

2aZnEt: $Zn(Et)_2$ (2.43 mL, 2.43 mmol, 1.0 M in hexanes) was added to a stirred solution of **2a** (440 mg, 1.16 mmol) in toluene (8 mL) and stirred at 100 °C overnight resulting in a clear solution. Upon slow cooling to room temperature **2aZn** (140 mg, 0.25 mmol, 21%) crystallized as clear colorless blocks.

^{1}H NMR (400 MHz, C_6D_6): δ (ppm) = 7.27 (d, J = 7.4 Hz, 4H, p-C_6H_3), 7.02 (t, J = 7.5 Hz, 2H, m-C_6H_3), 3.07 (t, J = 5.4 Hz, 4H, $NCH_2CH_2NC_6H_3$), 2.48 (s, 12H, $CH_3C_6H_3$), 3.35 (d, J = 8.8 Hz, 4H, NCH_2CH_2N), 2.13 (t, J = 5.4 Hz, 4H, $NCH_2CH_2NC_6H_3$), 1.99 (d, J = 8.8 Hz, 4H, NCH_2CH_2N), 1.32 (t, J = 8.0 Hz, 6H, $ZnCH_2CH_3$), 0.38 (q, J = 8.1 Hz, 4H, $ZnCH_2CH_3$); $^{13}C\{H\}$ NMR (101 MHz, C_6D_6): δ (ppm) = 154.9 (i-C_6H_3), 133.3 (o-C_6H_3), 129.3 (m-C_6H_3), 121.2 (p-C_6H_3), 62.3 ($NCH_2CH_2NC_6H_3$), 52.0 (NCH_2CH_2N), 48.0 ($NCH_2CH_2NC_6H_3$), 20.4 ($CH_3C_6H_3$), 12.3 ($ZnCH_2CH_3$), 3.6 ($ZnCH_2CH_3$); IR (ATR): $\tilde{\nu}$ [cm^{-1}] = 3052 (w), 2939 (w), 2893 (w), 2852 (w), 1585 (m), 1460 (m), 1418 (s), 1273 (s), 1087 (s), 955 (s), 755 (vs); anal. calc. (found) for $[C_{28}H_{44}Zn_2N_4]$: C 59.27 (59.59), H 7.82 (7.41), N 9.87 (9.70).

2aAlMe$_2$: $AlMe_3$ (2.00 mmol, 1.00 mL, 2.0 M in toluene) was added slowly to a stirred solution of **2a** (382 mg, 1.00 mmol) in toluene (10 mL) and stirred at reflux overnight. Upon slow cooling to room temperature **2aAlMe$_2$** (400 mg, 0.81 mmol, 81%) crystallized as clear colorless crystals.

^{1}H NMR (400 MHz, $CDCl_3$): δ (ppm) = 7.06 (d, J = 8.0 Hz, 4H, m-C_6H_3), 6.90 (t, J = 7.5 Hz, 2H, p-C_6H_3), 3.59 (d, J = 9.3 Hz, 4H, NCH_2CH_2N), 3.25 (t, J = 5.7 Hz, 4H, $NCH_2CH_2NC_6H_3$), 3.13 (t, J = 5.7 Hz, 4H, $NCH_2CH_2NC_6H_3$), 2.99 (d, J = 9.1 Hz, 4H, NCH_2CH_2N), 2.31 (s, 12H, $C_6H_3CH_3$), −0.74 (s, 12H, $Al(CH_3)_2$); $^{13}C\{^1H\}$ NMR (101 MHz, $CDCl_3$): δ (ppm) = 149.1 (i-C_6H_3), 137.8 (o-C_6H_3), 128.3 (m-C_6H_3), 123.2 (p-C_6H_3), 61.4 ($NCH_2CH_2NC_6H_3$), 51.7 ($NCH_2CH_2NC_6H_3$), 45.8 (NCH_2CH_2N), 19.0 ($C_6H_3CH_3$), −6.9 ($Al(CH_3)_2$); IR (ATR): $\tilde{\nu}$ [cm^{-1}] = 2935 (w), 2916 (w), 2838 (w), 2809 (w), 1466 (m), 1229 (m), 1184 (m), 1095 (m), 944 (m), 886 (m), 653 (s); anal. calc. (found) for $[C_{28}H_{47}N_4Al_2{\cdot}0.15\ C_7H_8]$: C 68.89 (68.96), H 9.39 (9.44), N 11.06 (11.22).

2bZn: $Zn(Et)_2$ (5.10 mL, 5.10 mmol, 1.0 M in hexanes) was added to a stirred solution of **2b** (930 mg, 2.43 mmol) in toluene (8 mL) and stirred at 100 °C overnight resulting in a clear solution. Upon slow cooling to room temperature **2bZn** (890 mg, 2.00 mmol, 82%) crystallized as clear colourless blocks.

^{1}H NMR (400 MHz, C_6D_6 + THF-d_8): δ (ppm) = 6.99 (d, J = 7.3 Hz, 4H, m-C_6H_3), 6.71 (t, J = 7.4 Hz, 2H, p-C_6H_3), 3.34–3.28 (m, 2H, $NCH_2CH_2NC_6H_3$), 2.83–2.77 (m, 2H, $NCH_2CH_2NC_6H_3$),

2.37–2.35 (m, 2H, NCH_2CH$_2$N), 2.28–2.17 (m, 4H, NCH_2CH$_2$NC$_6$H$_3$), 2.14–2.12 (m, 18H, NCH_3 + CH_3C$_6$H$_3$), 1.80–1.77 (m, 2H, NCH_2CH$_2$N); ^{13}C{H} NMR (101 MHz, C$_6$D$_6$ + THF-d_8): δ (ppm) = 156.9 (i-C_6H$_3$), 133.6 (*o*-C_6H$_3$), 128.6 (*m*-C_6H$_3$), 119.4 (*p*-C_6H$_3$), 61.2 (CH$_3$NCH_2CH_2NCH$_3$), 51.3 (NCH_2CH_2N), 50.1 (NCH_2CH_2N), 44.3 (CH_3NCH$_2$CH$_2$NCH_3), 20.4 (CH_3C$_6$H$_3$); IR (ATR): $\tilde{\nu}$ [cm^{-1}] = 3046 (w), 2966 (w), 2853 (w), 2836 (w), 1587 (m), 1469 (m), 1412 (m), 1279 (m), 1084 (m), 764 (vs), 740 (s); anal. calc. (found) for [C$_{24}$H$_{36}$ZnN$_4$]: C 64.64 (64.59), H 8.14 (7.70), N 12.56 (12.30).

2bAlH: A solution of **2b** (300 mg, 0.78 mmol) in Et$_2$O (10 mL) was cooled to −78 °C before it was added to AlH$_3$·NMe$_3$ (77 mg, 0.86 mmol) followed by stirring at room temperature overnight. The solvent was removed and the resulting crystalline solid was washed with *n*-pentane (2 × 5 mL) to obtain **2bAlH** (298 mg, 0.73 mmol, 93%) as a white crystalline solid.

^{1}H NMR (400 MHz, C$_6$D$_6$): δ (ppm) = 7.07–7.02 (m, 4H, *m*-C$_6$H$_3$), 6.97–6.93 (m, 2H, *p*-C$_6$H$_3$), 3.13–3.06 (m, 2H, NCH_2CH$_2$NC$_6$H$_3$), 2.61–2.50 (m, 4H, NCH_2CH$_2$N + NCH_2CH$_2$NC$_6$H$_3$), 2.46 (s, 6H, NCH_3), 2.11–2.04 (m, 2H, NCH_2CH$_2$N), 1.99 (s, 6H, C$_6$H$_3$CH_3), 1.96 (s, 6H, C$_6$H$_3$CH_3), 1.94–1.91 (m, 2H, NCH_2CH$_2$NC$_6$H$_3$), 1.77–1.70 (m, 2H, NCH_2CH$_2$NC$_6$H$_3$); ^{1}H NMR (400 MHz, CDCl$_3$): δ (ppm) = 6.75–6.66 (m, 6H, C$_6$H$_3$), 3.21–3.15 (m, 2H, NCH_2CH$_2$NC$_6$H$_3$), 3.08–2.98 (m, 4H, NCH_2CH$_2$N + NCH_2CH$_2$NC$_6$H$_3$), 2.83–2.75 (m, 2H, NCH_2CH$_2$N), 2.64–2.60 (m, 4H, NCH_2CH$_2$NC$_6$H$_3$), 2.55 (s, 6H, NCH$_3$), 2.10 (s, 6H, C$_6$H$_3$CH_3), 1.76 (s, 6H, C$_6$H$_3$CH_3); ^{13}C{^{1}H} NMR (101 MHz, C$_6$D$_6$): δ (ppm) = 153.0 (i-C_6H$_3$), 137.5 (*o*-C_6H$_3$), 128.4 (*m*-C_6H$_3$), 122.6 (*p*-C_6H$_3$), 58.8 (NCH$_2$CH_2NC$_6$H$_3$), 54.5 (NCH_2CH_2N), 47.8 (NCH_2CH$_2$NC$_6$H$_3$), 41.0 (NCH_3), 20.6 (C$_6$H$_3$CH_3), 18.5 (C$_6$H$_3$CH_3); IR (ATR): $\tilde{\nu}$ [cm^{-1}] = 2956 (w), 2910 (w), 2861 (w), 2806 (w), 1753 (w), 1590 (m), 1466 (m), 1339 (s), 1262 (s), 1217 (s), 1092 (s), 920 (m), 758 (vs), 654 (vs); anal. calc. (found) for [C24H37AlN4]: C 70.55 (69.93), H 9.13 (8.66), N 13.71 (13.42).

2bAlMe$_2$: AlMe$_3$ (15.7 mmol, 7.85 mL, 2.0 M in toluene) was added slowly to a stirred solution of **2b** (3.00 g, 7.80 mmol) in toluene (35 mL) and stirred under reflux overnight. After cooling to room temperature, the white suspension was filtered and the remaining white solid was dried in vacuum to obtain **2bAlMe$_2$** (2.73 g, 5.50 mmol, 70%). Crystals suitable for an XRD analysis grew from the filtrate upon standing at room temperature.

^{1}H NMR (400 MHz, CDCl$_3$): δ (ppm) = 7.07 (d, J = 7.4 Hz, 4H, *m*-C$_6$H$_3$), 6.91 (t, J = 7.4 Hz, 2H, *p*-C$_6$H$_3$), 3.48–3.30 (m, 6H, NCH_2CH$_2$N + NCH_2CH$_2$NC$_6$H$_3$), 3.01–2.87 (m, 6H, NCH_2CH$_2$N + NCH_2CH$_2$NC$_6$H$_3$), 2.71–2.69 (m, 6H, NCH_3), 2.32 (s, 12H, C$_6$H$_3$CH_3), −0.72–0.74 (m, 6H, Al(CH_3)$_2$), −0.79–0.81 (m, 6H, Al(CH_3)$_2$); ^{13}C{^{1}H} NMR (101 MHz, CDCl$_3$): δ (ppm) = 149.3 (i-C_6H$_3$), 138.0 (*o*-C_6H$_3$), 128.3 (*m*-C_6H$_3$), 123.2 (*p*-C_6H$_3$), 61.2 (NCH$_2$CH_2NC$_6$H$_3$), 54.2 (NCH_2CH_2N), 46.5 (NCH_2CH$_2$NC$_6$H$_3$), 40.3 (NCH_3), 18.9 (C$_6$H$_3$CH_3),–7.4 (Al(CH_3)$_2$), −9.00 (Al(CH_3)$_2$); IR (ATR): $\tilde{\nu}$ [cm^{-1}] = 2922 (w), 2796 (w), 1589 (vw), 1471 (m), 1263 (m), 1215 (m), 1107 (m), 953 (m), 886 (s), 769 (s), 648 (vs); anal. calc. (found) for [C$_{28}$H$_{48}$N$_4$Al$_2$·0.11 C$_7$H$_8$]: C 67.98 (68.68), H 9.78 (9.67), N 11.33 (11.35).

2dAlMe$_2$: AlMe$_3$ (5.00 mmol, 2.50 mL, 2.0 M in toluene) was added slowly to a stirred solution of **2d** (970 mg, 2.45 mmol) in toluene (20 mL) and stirred under reflux overnight. After cooling to room temperature, the solution was concentrated to about 6 mL to initiate crystallization. After standing at room temperature overnight **2dAlMe$_2$** (710 mg, 1.22 mmol, 50%) was isolated as clear colourless crystals.

^{1}H NMR (400 MHz, CDCl$_3$): δ (ppm) = 7.06 (d, J = 7.4 Hz, 4H, *m*-C$_6$H$_3$), 6.90 (t, J = 7.4 Hz, 2H, *p*-C$_6$H$_3$), 3.46–3.38 (m, 2H, NCH_2CH$_2$NC$_6$H$_3$), 3.33–3.25 (m, 2H, NCH_2CH$_2$CH$_2$N), 3.03–2.79 (m, 6H, NCH_2CH$_2$NC$_6$H$_3$ + NCH_2CH$_2$CH$_2$N), 2.67–2.61 (m, 8H, NCH_2CH$_2$NC$_6$H$_3$ + NCH_3), 2.32 (s, 12H, C$_6$H$_3$CH_3), 2.21–2.11 (m, 2H, CH$_2$CH$_2$CH$_2$) −0.78–0.81 (m, 12H, Al(CH_3)$_2$); ^{13}C{^{1}H} NMR (101 MHz, CDCl$_3$): δ (ppm) = 149.6 (i-C_6H$_3$), 138.1 (*o*-C_6H$_3$), 128.2 (*m*-C_6H$_3$), 123.0 (*p*-C_6H$_3$), 60.4/59.4 (NCH$_2$CH$_2$NC$_6$H$_3$), 56.4/56.1, (CH$_2$CH$_2$CH$_2$), 46.8/46.7 (NCH$_2$CH$_2$NC$_6$H$_3$), 40.2/40.0 (NCH$_3$), 22.6/20.4 (CH$_2$CH$_2$CH$_2$) 18.9/18.9 (C$_6$H$_3$CH$_3$), −8.0 /-9.0 (Al(CH$_3$)$_2$); IR (ATR): $\tilde{\nu}$ [cm^{-1}] = 2913 (w), 2812 (w), 1474 (m), 1422 (m), 1338 (m), 1236 (m), 1103 (m), 936 (m), 654 (vs), 566 (s); anal. calc. (found) for [C$_{29}$H$_{50}$N$_4$Al$_2$]: C 68.47 (68.50), H 9.91 (9.62), N 11.01 (10.85).

X-ray crystallography

The intensity data were collected on a GV-50 diffractometer with TitanS2 detector from Rigaku Oxford Diffraction (formerly Agilent Technologies) applying Cu-K$_\beta$ radiation (λ = 1.39222 Å) for **1mSnHMDS** and **1nZn** and Cu-K$_\alpha$ radiation (λ = 1.54184 Å) for all other compounds. Analytical absorption corrections were applied to the data.[23] The structures were solved by direct methods (SHELXT)[24] and refined by full-matrix least squares techniques against F_o^2 (SHELXL-2018).[25] The hydrogen atoms bonded to the Aluminium-ion of **1jAlH2**, **1kAlH2**, **2bAlH2** and to the amine groups of compound **2a** and **2b** were located by difference Fourier synthesis and refined isotropically. All other hydrogen atoms were included at calculated positions with fixed thermal parameters. All non-hydrogen atoms were refined anisotropically.[25] Crystallographic data as well as structure solution and refinement details are summarized in Table S1 of the ESI.† Olex2 was used for structure representations.[26]

Crystallographic data (excluding structure factors) has been deposited with the Cambridge Crystallographic Data Centre as supplementary publication CCDC-2026438 for **1jAlH$_2$**, CCDC-2026439 for **1kAlH$_2$**, CCDC-2026440 for **1mSnHMDS**, CCDC-2026441 for **1nMg**, CCDC-2026442 for **1nSnHMDS**, CCDC-2026443 for **1nZn**, CCDC-2026444 for **2a**, CCDC-2026430 for **2aAlMe$_2$**, CCDC-2026431 for **2aZnEt**, CCDC-2026432 for **2b**, CCDC-2026433 for **2bAlH**, CCDC-2026434 for **2bAlMe$_2$**, CCDC-2026435 for **2bMg**, CCDC-2026436 for **2bZn**, and CCDC-2026437 for **2dAlMe$_2$**.†

Conflicts of interest

There are no conflicts to declare.

Acknowledgements

The work is dedicated to Winfried Plass on the occasion of his 60th birthday. The project was financially supported by the Deutsche Forschungsgemeinschaft (DFG, KR4782/3-1), the Friedrich Schiller University Jena and the *Elite Network of Bavaria*. We thanks the reviewers for valuable comments and suggestions.

Notes and references

1 (*a*) R. Robson, *Inorg. Nucl. Chem. Lett.*, 1970, **6**, 125; (*b*) R. Robson, *Aust. J. Chem.*, 1970, **23**, 2217; (*c*) N. H. Pilkington and R. Robson, *Aust. J. Chem.*, 1970, **23**, 2225; (*d*) A. E. Allen and D. W. C. Macmillan, *Chem. Sci.*, 2012, **2012**, 633; (*e*) I. Bratko and M. Gomez, *Dalton Trans.*, 2013, **42**, 10664; (*f*) J. A. Mata, F. E. Hahn and E. Peris, *Chem. Sci.*, 2014, **5**, 1723; (*g*) P. Buchwalter, J. Rosé and P. Braunstein, *Chem. Rev.*, 2015, **115**, 28; (*h*) R. Kretschmer, *Chem. – Eur. J.*, 2020, **26**, 2099–2119.

2 (*a*) R. E. Mulvey, *Organometallics*, 2006, **25**, 1060; (*b*) *Cooperative Catalysis: Designing Efficient Catalysts for Synthesis*, ed. R. Peters, Wiley, 2015; (*c*) P. Kalck, *Homo- and Heterobimetallic Complexes in Catalysis*, Springer International Publishing, Cham, 2016, vol. 59; (*d*) L. Tebben, C. Mück-Lichtenfeld, G. Fernández, S. Grimme and A. Studer, *Chem. – Eur. J.*, 2017, **23**, 5864; (*e*) R. E. Mulvey, *Acc. Chem. Res.*, 2009, **42**, 743; (*f*) S. D. Robertson, M. Uzelac and R. E. Mulvey, *Chem. Rev.*, 2019, **119**, 8332.

3 (*a*) P. P. Power, *Nature*, 2010, **463**, 171; (*b*) S. Yadav, S. Saha and S. S. Sen, *ChemCatChem*, 2016, **8**, 486; (*c*) R. Rochat, M. J. Lopez, H. Tsurugi and K. Mashima, *ChemCatChem*, 2016, **8**, 10; (*d*) M. S. Hill, D. J. Liptrot and C. Weetman, *Chem. Soc. Rev.*, 2016, **45**, 972; (*e*) S. Dagorne and R. Wehmschulte, *ChemCatChem*, 2018, **10**, 2509; (*f*) C. Weetman and S. Inoue, *ChemCatChem*, 2018, **10**, 4213–4228; (*g*) L. C. Wilkins and R. L. Melen, *Coord. Chem. Rev.*, 2016, **324**, 123; (*h*) S. Harder, *Early Main Group Metal Catalysis. Concepts and Reactions*, John Wiley & Sons, Incorporated, Newark, 2020.

4 A. Röther and R. Kretschmer, *J. Organomet. Chem.*, 2020, **918**, 121289.

5 (*a*) R. T. Boeré, R. T. Oakley and R. W. Reed, *J. Organomet. Chem.*, 1987, **331**, 161; (*b*) D. Lindauer, R. Beckert, M. Döring, P. Fehling and H. Görls, *J. Prakt. Chem.*, 1995, **337**, 143; (*c*) J. R. Hagadorn and J. Arnold, *Angew. Chem., Int. Ed.*, 1998, **37**, 1729; (*d*) J. R. Babcock, C. Incarvito, A. L. Rheingold, J. C. Fettinger and L. R. Sita, *Organometallics*, 1999, **18**, 5729; (*e*) G. D. Whitener, J. R. Hagadorn and J. Arnold, *J. Chem. Soc., Dalton Trans.*, 1999, 1249; (*f*) S. Bambirra, A. Meetsma, B. Hessen and J. H. Teuben, *Organometallics*, 2001, **20**, 782; (*g*) C.-T. Chen, L. H. Rees, A. R. Cowley and M. L. H. Green, *J. Chem. Soc., Dalton Trans.*, 2001, 1761; (*h*) H. Kawaguchi and T. Matsuo, *Chem. Commun.*, 2002, 958; (*i*) J.-F. Li, L.-H. Weng, X.-H. Wei and D.-S. Liu, *J. Chem. Soc., Dalton Trans.*, 2002, 1401; (*j*) H. A. Jenkins, D. Abeysekera, D. A. Dickie and J. A. C. Clyburne, *J. Chem. Soc., Dalton Trans.*, 2002, 3919; (*k*) C.-T. Chen, C.-A. Huang, Y.-R. Tzeng and B.-H. Huang, *Dalton Trans.*, 2003, 2585; (*l*) J. Grundy, M. P. Coles and P. B. Hitchcock, *J. Organomet. Chem.*, 2002, **662**, 178; (*m*) B. Clare, N. Sarker, R. Shoemaker and J. R. Hagadorn, *Inorg. Chem.*, 2004, **43**, 1159; (*n*) M. S. Hill, P. B. Hitchcock and S. M. Mansell, *Dalton Trans.*, 2006, 1544; (*o*) S.-D. Bai, J.-P. Guo and D.-S. Liu, *Dalton Trans.*, 2006, 2244; (*p*) S.-D. Bai, J.-P. Guo, D.-S. Liu and W.-Y. Wong, *Eur. J. Inorg. Chem.*, 2006, **2006**, 4903; (*q*) M. Ohashi, A. Yagyu, T. Yamagata and K. Mashima, *Chem. Commun.*, 2007, 3103; (*r*) Z. Lu, N. J. Hill, M. Findlater and A. H. Cowley, *Inorg. Chim. Acta*, 2007, **360**, 1316; (*s*) M. V. Yakovenko, A. V. Cherkasov, G. K. Fukin, D. Cui and A. A. Trifonov, *Eur. J. Inorg. Chem.*, 2010, **2010**, 3290; (*t*) K. Stippich, R. Kretschmer, R. Beckert and H. Goerls, *Synthesis*, 2010, 1311; (*u*) A. O. Tolpygin, A. S. Shavyrin, A. V. Cherkasov, G. K. Fukin and A. A. Trifonov, *Organometallics*, 2012, **31**, 5405; (*v*) G. G. Skvortsov, G. K. Fukin, S. Y. Ketkov, A. V. Cherkasov, K. A. Lyssenko and A. A. Trifonov, *Eur. J. Inorg. Chem.*, 2013, **2013**, 4173; (*w*) S.-D. Bai, R.-Q. Liu, T. Wang, F. Guan, Y.-B. Wu, J.-B. Chao, H.-B. Tong and D.-S. Liu, *Polyhedron*, 2013, **65**, 161; (*x*) A. O. Tolpygin, G. G. Skvortsov, A. V. Cherkasov, G. K. Fukin, T. A. Glukhova and A. A. Trifonov, *Eur. J. Inorg. Chem.*, 2013, **2013**, 6009; (*y*) M. Bayram, D. Bläser, C. Wölper and S. Schulz, *Organometallics*, 2014, **33**, 2080; (*z*) A. O. Tolpygin, A. V. Cherkasov, G. K. Fukin and A. A. Trifonov, *Inorg. Chem.*, 2014, **53**, 1537; (*aa*) M. V. Yakovenko, N. Y. Udilova, T. A. Glukhova, A. V. Cherkasov, G. K. Fukin and A. A. Trifonov, *New J. Chem.*, 2015, **39**, 1083; (*ab*) M. Stollenz, J. E. Raymond, L. M. Pérez, J. Wiederkehr and N. Bhuvanesh, *Chem. – Eur. J.*, 2016, **22**, 2396; (*ac*) N. Kazeminejad, D. Munzel, M. T. Gamer and P. W. Roesky, *Chem. Commun.*, 2017, **53**, 1060; (*ad*) C. O'Dea, O. Ugarte Trejo, J. Arras, A. Ehnbom, N. Bhuvanesh and M. Stollenz, *J. Org. Chem.*, 2019, **84**, 14217; (*ae*) A. Rösch, S. H. F. Schreiner, P. Schüler, H. Görls and R. Kretschmer, *Dalton Trans.*, 2020, **49**, DOI: 10.1039/D0DT01923B, accepted for publication.

6 (*a*) S. Herres-Pawlis, A. Neuba, O. Seewald, T. Seshadri, H. Egold, U. Flörke and G. Henkel, *Eur. J. Org. Chem.*, 2005, **2005**, 4879; (*b*) G. Jin, C. Jones, P. C. Junk, K.-A. Lippert, R. P. Rose and A. Stasch, *New J. Chem.*, 2009, **33**, 64; (*c*) X. Zhang, C. Wang, M. Xue, Y. Zhang, Y. Yao and Q. Shen, *J. Organomet. Chem.*, 2012, **713**, 182; (*d*) X. Zhang, C. Wang, M. Xue, Y. Zhang, Y. Yao and Q. Shen, *J. Organomet. Chem.*, 2012, **716**, 86; (*e*) C. Wang, X. Zhang, M. Xue, Y. Zhang and Q. Shen, *Organometallics*, 2013, **32**, 3618; (*f*) C. Wang, X. Zhang, M. Xue, Y. Zhang and Q. Shen, *Dalton Trans.*, 2013, **42**, 7009; (*g*) J. Stanek, T. Rösener, A. Metz, J. Mannsperger, A. Hoffmann and S. Herres-Pawlis, in *Topics in Heterocyclic Chemistry*, Springer Berlin

Heidelberg, Berlin, Heidelberg, 2015; (*h*) V. Vass, M. Dehmel, F. Lehni and R. Kretschmer, *Eur. J. Org. Chem.*, 2017, **2017**, 5066; (*i*) M. Dehmel, V. Vass, L. Prock, H. Görls and R. Kretschmer, *Inorg. Chem.*, 2020, **59**, 2733.

7 (*a*) D. V. Vitanova, F. Hampel and K. C. Hultzsch, *Dalton Trans.*, 2005, 1565; (*b*) D. V. Vitanova, F. Hampel and K. C. Hultzsch, *J. Organomet. Chem.*, 2005, **690**, 5182; (*c*) M. F. Pilz, C. Limberg and B. Ziemer, *J. Org. Chem.*, 2006, **71**, 4559; (*d*) M. F. Pilz, C. Limberg, S. Demeshko, F. Meyer and B. Ziemer, *Dalton Trans.*, 2008, 1917; (*e*) D. F.-J. Piesik, S. Range and S. Harder, *Organometallics*, 2008, **27**, 6178; (*f*) S. Gong, H. Ma and J. Huang, *Dalton Trans.*, 2009, 8237; (*g*) D. F.-J. Piesik, R. Stadler, S. Range and S. Harder, *Eur. J. Inorg. Chem.*, 2009, **2009**, 3569; (*h*) J. P. Falkenhagen, P. Haack, C. Limberg and B. Braun, *Z. Anorg. Allg. Chem.*, 2011, **637**, 1741; (*i*) I. El-Zoghbi, T. J. J. Whitehorne and F. Schaper, *Dalton Trans.*, 2013, **42**, 9376; (*j*) S. Sun, Q. Sun, B. Zhao, Y. Zhang, Q. Shen and Y. Yao, *Organometallics*, 2013, **32**, 1876; (*k*) L. Li, C. Wu, D. Liu, S. Li and D. Cui, *Organometallics*, 2013, **32**, 3203; (*l*) J. Intemann, M. Lutz and S. Harder, *Organometallics*, 2014, **33**, 5722; (*m*) M. E. Desat, S. Gärtner and R. Kretschmer, *Chem. Commun.*, 2017, **53**, 1510; (*n*) A. Phanopoulos, A. H. M. Leung, S. Yow, D. Palomas, A. J. P. White, K. Hellgardt, A. Horton and M. R. Crimmin, *Dalton Trans.*, 2017, **46**, 2081; (*o*) A. Phanopoulos, M. Warren, A. J. P. White, A. Horton and M. R. Crimmin, *Dalton Trans.*, 2017, **46**, 2077; (*p*) M. E. Desat and R. Kretschmer, *Chem. – Eur. J.*, 2018, **24**, 12397–12404; (*q*) M. E. Desat and R. Kretschmer, *Inorg. Chem.*, 2019, **58**, 16302–16311; (*r*) M. E. Desat and R. Kretschmer, *Dalton Trans.*, 2019, **48**, 17718–17722; (*s*) M. E. Desat and R. Kretschmer, *Z. Anorg. Allg. Chem.*, 2020, **646**, 625–630.

8 C. Camp and J. Arnold, *Dalton Trans.*, 2016, 14462–14498.

9 (*a*) R. Kretschmer, M. Dehmel and M. Bodensteiner, *Eur. J. Inorg. Chem.*, 2017, **2017**, 965; (*b*) N. A. Phillips, J. O'Hanlon, T. N. Hooper, A. J. P. White and M. R. Crimmin, *Org. Lett.*, 2019, **21**, 7289.

10 M. L. Hlavinka and J. R. Hagadorn, *Chem. Commun.*, 2003, 2686.

11 (*a*) M. L. Hlavinka and J. R. Hagadorn, *Organometallics*, 2005, **24**, 5335; (*b*) M. L. Hlavinka and J. R. Hagadorn, *Organometallics*, 2005, **24**, 4116; (*c*) L. E. Garner, H. Zhu, M. L. Hlavinka, J. R. Hagadorn and E. Y.-X. Chen, *J. Am. Chem. Soc.*, 2006, **128**, 14822; (*d*) M. L. Hlavinka and J. R. Hagadorn, *Organometallics*, 2006, **25**, 3501; (*e*) M. L. Hlavinka, M. J. McNevin, R. Shoemaker and J. R. Hagadorn, *Inorg. Chem.*, 2006, **45**, 1815.

12 N. Millot, C. C. Santini, B. Fenet and J. M. Basset, *Eur. J. Inorg. Chem.*, 2002, **2002**, 3328.

13 C. M. Herzog, Master Thesis "Synthese und Charakterisierung von Bis(amidoamin)liganden sowie deren Umsetzung zu dinuklearen Gruppe 13-Elementverbindungen", Universität Regensburg, 2016.

14 M. Ostermeier, C. Limberg, C. Herwig and B. Ziemer, *Z. Anorg. Allg. Chem.*, 2009, **635**, 1823.

15 (*a*) H. V. R. Dias, W. Jin and R. E. Ratcliff, *Inorg. Chem.*, 1995, **34**, 6100; (*b*) N. Kuhn, S. Fuchs and M. Steimann, *Z. Anorg. Allg. Chem.*, 2000, **626**, 1387; (*c*) W. Uhl and B. Jana, *Chem. – Eur. J.*, 2008, **14**, 3067; (*d*) B. Lyhs, D. Bläser, C. Wölper and S. Schulz, *Chem. – Eur. J.*, 2011, **17**, 4914; (*e*) Y. Yang, H. P. Li, C. Wang and H. W. Roesky, *Inorg. Chem.*, 2012, **51**, 2204; (*f*) Z. Yang, M. Zhong, X. Ma, K. Nijesh, S. De, P. Parameswaran and H. W. Roesky, *J. Am. Chem. Soc.*, 2016, **138**, 2548; (*g*) A. R. Leverett, V. Diachenko, M. L. Cole and A. I. McKay, *Dalton Trans.*, 2019, **48**, 13197; (*h*) C. G. Gianopoulos, K. Kirschbaum and M. R. Mason, *Organometallics*, 2014, **33**, 4503.

16 A. Caise, D. Jones, E. L. Kolychev, J. Hicks, J. M. Goicoechea and S. Aldridge, *Chem. – Eur. J.*, 2018, **24**, 13624.

17 (*a*) S. R. Foley, G. P. A. Yap and D. S. Richeson, *Organometallics*, 1999, **18**, 4700; (*b*) P. B. Hitchcock, J. Hu, M. F. Lappert and J. R. Severn, *Dalton Trans.*, 2004, 4193; (*c*) I. A. Guzei, V. I. Timokhin and R. West, *Acta Crystallogr., Sect. C: Cryst. Struct. Commun.*, 2006, **62**, m90–m92; (*d*) Z.-Y. Chai and Z.-X. Wang, *Dalton Trans.*, 2009, 8005; (*e*) M. K. Barman, A. Baishya, T. Peddarao and S. Nembenna, *J. Organomet. Chem.*, 2014, **772–773**, 265.

18 (*a*) W.-P. Leung, K.-P. Chan, K.-W. Kan and T. C. W. Mak, *Organometallics*, 2008, **27**, 2767; (*b*) S. Krupski, J. V. Dickschat, A. Hepp, T. Pape and F. E. Hahn, *Organometallics*, 2012, **31**, 2078; (*c*) R. K. Raut, P. Sahoo, D. Chimnapure and M. Majumdar, *Dalton Trans.*, 2019, **48**, 10953.

19 (*a*) F. Dannenberg, G. Thiele, S. Dehnen and M. Mehring, *Z. Anorg. Allg. Chem.*, 2017, **643**, 360; (*b*) I. D'auria, M. C. D'Alterio, C. Tedesco and C. Pellecchia, *RSC Adv.*, 2019, **9**, 32771; (*c*) G. Ballmann, S. Grams, H. Elsen and S. Harder, *Organometallics*, 2019, **38**, 2824.

20 (*a*) W.-P. Leung, C.-W. So, K.-H. Chong, K.-W. Kan, H.-S. Chan and T. C. W. Mak, *Organometallics*, 2006, **25**, 2851; (*b*) C.-Y. Lin, C.-F. Tsai, H.-J. Chen, C.-H. Hung, R.-C. Yu, P.-C. Kuo, H. M. Lee and J.-H. Huang, *Chem. – Eur. J.*, 2006, **12**, 3067; (*c*) S. G. Alexander, M. L. Cole, C. M. Forsyth, S. K. Furfari and K. Konstas, *Dalton Trans.*, 2009, 2326; (*d*) B. Goswami, R. Yadav, C. Schoo and P. W. Roesky, *Dalton Trans.*, 2020, **49**, 675; (*e*) M. L. Cole, A. J. Davies, C. Jones, P. C. Junk, A. I. McKay and A. Stasch, *Z. Anorg. Allg. Chem.*, 2015, **641**, 2233.

21 B. Nekoueishahraki, H. W. Roesky, G. Schwab, D. Stern and D. Stalke, *Inorg. Chem.*, 2009, **48**, 9174.

22 R. S. Cahn, C. Ingold and V. Prelog, *Angew. Chem., Int. Ed. Engl.*, 1966, **5**, 385.

23 *CrysAlisPro, version 171.38.42b*, Agilent Technologies Inc., Oxford, GB, 2015.

24 G. M. Sheldrick, *Acta Crystallogr., Sect. A: Found. Adv.*, 2015, **71**, 3.

25 G. M. Sheldrick, *Acta Crystallogr., Sect. C: Struct. Chem.*, 2015, **71**, 3.

26 O. V. Dolomanov, L. J. Bourhis, R. J. Gildea, J. A. K. Howard and H. Puschmann, *J. Appl. Crystallogr.*, 2009, **42**, 339.